ChemPubSoc Europe

DOI: 10.1002/chem.201805665

CHEMISTRY A European Journal Full Paper

Bioinorganic Chemistry

Activation and Photoinduced Release of Alkynes on a Biomimetic Tungsten Center: The Photochemical Behavior of the W—S-Phoz System

Lydia M. Peschel[+],[a] Carina Vidovič[+],[a] Ferdinand Belaj,[a] Dmytro Neshchadin,*[b] and Nadia C. Mösch-Zanetti*[a]

Abstract: The synthesis and structural determination of four tungsten alkyne complexes coordinated by the bio-inspired S,N-donor ligand 2-(4′,4′-dimethyloxazoline-2′-yl)thiophenolate (S-Phoz) is presented. A previously established protocol that involved the reaction of the respective alkyne with the bis-carbonyl precursor $[W(CO)_2(S\text{-}Phoz)_2]$ was used for the complexes $[W(CO)(C_2R_2)(S\text{-}Phoz)_2]$ (R = H, **1a**; Me, **1b**; Ph, **1c**). Oxidation with pyridine-*N*-oxide gave the corresponding W-oxo species $[WO(C_2R_2)(S\text{-}Phoz)_2]$ (R = H, **2a**; Me, **2b**; Ph, **2c**). All W-oxo-alkyne complexes (**2a**, **b**, **c**) were found to be capable of alkyne release upon light irradiation to afford five-coordinate $[WO(S\text{-}Phoz)_2]$ (**3**). The photoinduced release of the alkyne ligand was studied in detail by in situ ^{1}H NMR measurements, which revealed correlation of the photodissociation rate constant (**2b** > **2a** > **2c**) with the elongation of the alkyne C≡C bond in the molecular structures. Oxidation of $[WO(S\text{-}Phoz)_2]$ (**3**) with pyridine-*N*-oxide yielded $[WO_2(S\text{-}Phoz)_2]$ (**4**), which shows highly fluxional behavior in solution. Variable-temperature ^{1}H NMR spectroscopy revealed three isomeric forms with respect to the ligand arrangement versus each other. Furthermore, compound **4** rearranges to tetranuclear oxo compound $[W_4O_4(\mu\text{-}O)_6(S\text{-}Phoz)_4]$ (**5**) and dinuclear $[\{WO(\mu\text{-}O)(S\text{-}Phoz)\}_2]$ (**6**) over time. The latter two were identified by single-crystal X-ray diffraction analyses.

Introduction

Tungsten is the only third-row transition metal that occurs in native enzymes. It is used by the unique W-dependent enzyme acetylene hydratase (AH) for the catalysis of the net hydration of acetylene (ethyne, C_2H_2) to acetaldehyde (CH_3CHO).[1,2] The molecular structure of AH has been solved and shows a W^{IV} center in a sulfur-rich environment created by two molybdopterin moieties, a cysteine, and an oxygen ligand, which is believed to be water (Figure 1).[3,4] Several proposals on how the two substrates, water and acetylene, react with each other at the active site of AH have been discussed. While the debate is ongoing, DFT and QM/MM calculations favor a first-shell mechanism, in which the C_2H_2 substrate is activated by the W^{IV} center by formation of a side-on (η^2) adduct.[4,5]

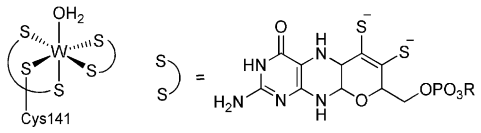

Figure 1. Active site of acetylene hydratase.[4]

Biomimetic model chemistry of Mo- and W-dependent enzymes has been extensively explored.[6,7] As the metal center is held in its active site by coordination to the dithiolene moiety of the molybdopterin cofactor, complexes with dithiolene-type ligands (e.g., malonitrile) have been developed.[7,8] Nevertheless, non-dithiolene ligands have likewise been introduced, such as the N_3-donor hydridotris(3,5-dimethyl-1-pyrazolyl)borate) (Tp′),[9] the S_2,N-donor 2,6-bis(2,2-diphenyl-2-thioethyl)pyridinate,[10] the S,N-donor 2-pyridyldiphenyl-methanethiolate,[11] or the S_2,N_2-donor *N*,*N*′-dimethyl-*N*,*N*′-bis(2-thiolatophenyl)ethylenediamine.[12]

On the other hand, biomimetic model chemistry specifically for AH is virtually unexplored. The only structural-functional model $[Et_4N]_2[WO(mnt)_2]$ (mnt = malonitrile), originally designed to mimic W-dependent aldehyde ferredoxin oxidore-

[a] Dr. L. M. Peschel,[+] C. Vidovič,[+] Dr. F. Belaj, Prof. N. C. Mösch-Zanetti
Institute of Chemistry, University of Graz
Schubertstrasse 1, 8010 Graz (Austria)
E-mail: nadia.moesch@uni-graz.at

[b] Dr. D. Neshchadin
Institute of Physical and Theoretical Chemistry
Graz University of Technology
Stremayrgasse 9, 8010 Graz (Austria)
E-mail: neshchadin@tugraz.at

[+] These authors contributed equally to this work.

Supporting information and the ORCID identification number(s) for the author(s) of this article can be found under: https://doi.org/10.1002/chem.201805665.

ductase, was reported to perform approximately nine turnovers of C_2H_2 hydration.[13] However, a recent report questioned the reproducibility of catalytic acetaldehyde formation by $[Et_4N]_2[WO(mnt)_2]$.[14] Furthermore, the malonitrile system did not allow isolation of W–C_2H_2 adducts, although it was suggested by theoretical calculations on $[WO(mnt)_2]^{2-}$.[13,18]

In general, tungsten compounds with a coordinated molecule of acetylene are extremely rare with only three systems being considered models for AH. Although they were not designed as models, the tungsten dithiocarbamate complexes $[W(CO)(C_2H_2)(dtc)_2]$ and $[WO(C_2H_2)(dtc)_2]$ (dtc = S_2CNMe_2, S_2CNEt_2) were used to study the coordination of alkynes in general (Figure 2, left).[17,19] Scorpionate complexes $[W(CO)(C_2H_2)Tp'I]$, $[WO(C_2H_2)Tp'I]$, and $[WO(C_2H_2)(H_2O)Tp'][OTf]$ were found to form tungsten-vinyl and -vinylidene compounds (Figure 2, middle).[16,20,21]

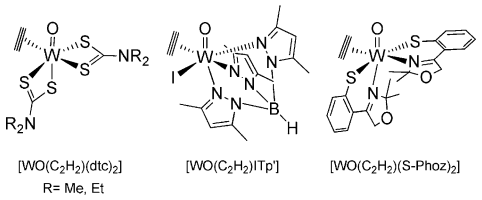

Figure 2. Structural models of AH.[15–17]

Recently, we have reported a model system specifically designed for AH by using the bio-inspired S-Phoz ligand (S-Phoz = 2-(4′,4′-dimethyloxazoline-2′-yl)thiophenolate, Figure 2, right).[15,22,23] The thiophenolate donors are considered to resemble the anionic S-donors of the natural pterin cofactor. Oxazoline moieties are naturally occurring[24] and have been shown to be versatile in transition-metal coordination chemistry and catalysis.[25] This fruitful combination of the biologically relevant S-donor and the versatile oxazoline allowed the development of W–C_2H_2 adducts to include the W^{IV}-oxo-ethyne compound with the metal being in the biologically relevant +IV oxidation state, which was established for the first time by X-ray diffraction analysis. Furthermore, with $[WO(C_2H_2)(S\text{-}Phoz)_2]$, we could demonstrate reversible activation of acetylene by light,[15] a process which has not been reported previously.

In general, mononuclear compounds of the type $[W(CO)(RC_2R')L_n]$ can be obtained through two synthetic routes: a) prevailingly, by reacting precursors of the type $[W(CO)(RC_2R')_2(MeCN)X_2]$, $[W(CO)(RC_2R')_2(2,2'\text{-bipy})X]X$, or $[W(CO)(RC_2R')L_2X_2]$[26] (X = Cl, Br, I) with appropriate ligands L_n or b) by introducing the ligands first to form intermediate $[W(CO)_mL_n]$ complexes, and subsequent substitution of CO by the alkyne. Strategy a) has been described for alkynes with R ≠ R′ ≠ H,[27] but as precursors with unsubstituted acetylene groups are not accessible, only method b) is applicable for the preparation of C_2H_2 complexes.

Herein, we report a detailed description of the W–S-Phoz system and its reactivity towards alkynes and oxygen atom transfer agents and show that the alkyne scope can easily be extended from ethyne to 2-butyne (dimethylacetylene, C_2Me_2) and 1,2-diphenylethyne (diphenylacetylene, C_2Ph_2). This brings further insights into the photochemistry of alkyne complexes and helps to reveal the basic underlying principles.

Results and Discussion

Synthesis of alkyne complexes

$[W(CO)(C_2Me_2)(S\text{-}Phoz)_2]$ (**1b**) and $[W(CO)(C_2Ph_2)(S\text{-}Phoz)_2]$ (**1c**) were synthesized from $[W(CO)_2(S\text{-}Phoz)_2]$[15,23] in yields of 76 and 67%, respectively (Scheme 1). Formation of the product is accompanied by a gradual color change from deep orange to green (**1b**) or brownish-green (**1c**). The oily crude products were purified by dissolving them in dichloromethane and stirring with silica. After filtration and precipitation with heptane, the products were obtained as microcrystalline materials.

Under the exclusion of light, oxidation with pyridine-*N*-oxide (Py*N*O) yielded the desired oxo compounds $[WO(C_2Me_2)(S\text{-}Phoz)_2]$ (**2b**) and $[WO(C_2Ph_2)(S\text{-}Phoz)_2]$ (**2c**) in a fast reaction, which was evidenced by CO evolution, a color change to yellow, and a characteristic pyridine odor. The microcrystalline, pale yellow products were obtained after recrystallization in 65 and 62% yield, respectively. Compounds $[W(CO)(C_2H_2)(S\text{-}Phoz)_2]$ (**1a**) and $[WO(C_2H_2)(S\text{-}Phoz)_2]$ (**2a**) were both prepared as previously reported.[15] Under an inert atmosphere, all compounds are stable for several months without decomposition. The CO compounds **1a**–**c** are highly soluble in polar solvents, especially in dichloromethane, and in toluene. The solubility of the oxo compounds **2a**–**c** is significantly lowered. Additionally, they were found to be only sparingly soluble in acetonitrile, which can be exploited during workup. As previously observed for $[W(CO)(C_2H_2)(S\text{-}Phoz)_2]$ (**1a**),[15] NMR spectroscopy in CD_2Cl_2 revealed the presence of two isomers of $[W(CO)(C_2Me_2)(S\text{-}Phoz)_2]$ (**1b**, 5:95) and $[W(CO)(C_2Ph_2)(S\text{-}Phoz)_2]$ (**1c**, 45:55) with respect to the relative orientation of the S,N-ligand (Scheme 1). For complex **1b**, a clear preference for the *N*,*N*-*trans* configura-

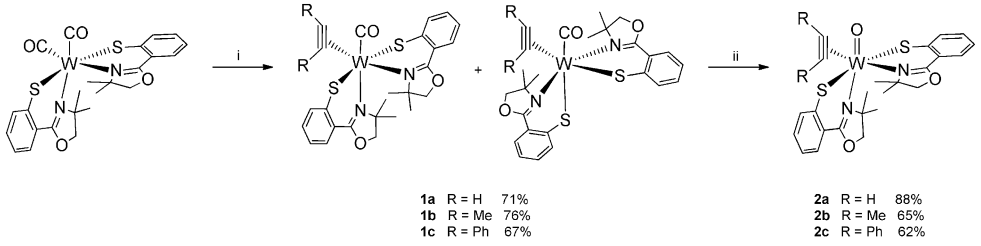

Scheme 1. Syntheses: i) 5.0 equiv. C_2Me_2/C_2Ph_2 or > 2.0 equiv. C_2H_2, CH_2Cl_2, heated at reflux, isomeric mixtures in solution; ii) 1.1 equiv. PyNO, CH_2Cl_2, RT.[15]

tion was observed, whereas for complex **1c**, a highly dynamic behavior was demonstrated (see below). In the ^{1}H NMR spectra of all W–S-Phoz complexes, the oxazoline CH_2 resonances are particularly indicative. In the bis-CO starting material $[W(CO)_2(S\text{-}Phoz)_2]$, they are found at 3.9 and 2.8 ppm, whereas in complexes **1b** and **1c**, a loss of symmetry and significant deshielding are observed, which shifts the resonances in the region between 4.3 and 3.8 ppm. The introduction of the oxo group (**2b**,**c**) causes the resonances to spread between 3.9 and 1.9 ppm. In complex **2b**, the methyl resonances of 2-butyne are found at 3.1 and 3.0 ppm, whereas in complex **1b**, they are at 2.9 and 2.5 ppm, which indicates less electron density on its methyl groups in the oxo compound. The coordination of the alkyne ligand to the W center hinders rotation around the W–alkyne bond, and thus, the compounds lose their C2 symmetry. Two-dimensional NMR spectroscopy and ^{13}C–^{183}W couplings in the ^{13}C NMR spectra were used to identify the C≡C resonances (Table 1). These resonances have previously been used to estimate the formal alkyne electron donation number.[27] According to this concept the shifts in the carbonyl complexes **1b** and **1c** (211 to 192 ppm) indicate a four-electron donation. In the case of the oxo species **2b** and **2c**, the resonances (148 to 159 ppm) are in the typical region for three-electron donation in bis-alkyne systems. In rare cases, shifts as low as 137 ppm have been previously attributed to four-electron donation;[28] hence, four-electron donation is proposed for these complexes. The drastic shifts are believed to originate from a reduced ability for π-backdonation from the W center upon oxidation, which causes a weaker coordination, and thus, leaves more electron density on the alkyne carbon atoms.

Solid-state IR spectra exhibit a single C≡O stretch for complex **1b** (bulk material) and single crystals of complex **1c** and two resonances for complex **1c** as bulk material (Table 1, see below). Oxidation is evidenced by distinct W=O bands at 934 (**2b**) and 936 cm^{-1} (**2c**). The alkyne C≡C stretches are found between 1620 and 1500 cm^{-1} and were assigned only tentatively as the C=N stretch of S-Phoz is found in the same region.

Treatment of the model complex $[WO(C_2H_2)(S\text{-}Phoz)_2]$ (**2a**) with 1 equivalent of degassed water in $CDCl_3$ (10 μL of a stock solution of 14 μL H_2O in 200 μL $CDCl_3$) resulted in decomposition of the complex. The added water quantitatively protonated the ligand to lead to a 2:1 ratio of free ligand HS-Phoz and intact complex **2a**. Also, complex **2b** was treated with the aqueous stock solution, and the reaction was monitored by ^{1}H NMR spectroscopy, but as for complex **2a**, hydrolysis predominantly occurred and no typical multiplet peaks of the water-addition product could be observed. Although the hydration might occur, the observation of it is hampered by the fast hydrolysis. Nevertheless, the synthesis of our structural model is important as it provides much-needed information on basic tungsten acetylene chemistry in higher oxidation states and will help the development of future systems that are more resistant towards the aqueous enzyme conditions.

Dynamic behavior of $[W(CO)(C_2Ph_2)(S\text{-}Phoz)_2]$ (1c)

As mentioned above, NMR spectroscopy revealed the presence of two isomers of $[W(CO)(C_2Ph_2)(S\text{-}Phoz)_2]$ (**1c**) in solution (45:55 in CD_2Cl_2). To date, all obtained solid-state structures of W–S-Phoz complexes revealed the *S,S-trans* or *N,N-trans* isomers (see below). The conceivable *S,N-trans* isomer has never been observed. Several crystals of complex **1c** were picked, and their molecular structure or unit cells and IR spectra were determined (IR: $\tilde{\nu}(CO) = 1927\ cm^{-1}$). All showed that only the *S,S-trans* isomer crystallizes as single crystals. Microcrystalline products, on the other hand, were identified as isomeric mixtures (IR: $\tilde{\nu}(CO) = 1927, 1894\ cm^{-1}$). Redissolving single crystals afforded the initially observed 45:55 *S,S-/N,N-trans* mixture in CD_2Cl_2, whereas in other solvents, such as $CDCl_3$, [D_6]DMSO, [D_8]THF, C_6D_6, and [D_3]MeCN, isomeric ratios ranging from 20:80 to 47:53 were observed. This suggests a dynamic equilibrium in solution that is dependent on the solvent.

This behavior highlights the flexibility and adaptability of the S-Phoz system. The required *hemi*-lability and capability to coordinate in κ^1- and κ^2-fashion have been demonstrated previously.[29] Similar steps have been proposed to explain the dynamic behavior of dithiocarbamate and dithiophosphinate W–alkyne complexes.[17,30] The dynamic behavior seen in complex **1c** is also likely to occur in complexes **1a** and **1b**, although less pronounced, because a clear preference for one isomer, most likely *N,N-trans*, is observed. Nevertheless, it explains why both isomeric forms of the W–carbonyl species converge to the isomerically pure W–oxo species $[WO(C_2R_2)(S\text{-}Phoz)_2]$ (**2a**–**c**).

Table 1. Selected ^{13}C NMR (CD_2Cl_2) and IR data of $[W(CO)(C_2R_2)(S\text{-}Phoz)_2]$ and $[WO(C_2R_2)(S\text{-}Phoz)_2]$ complexes.

		^{13}C NMR				IR			Ref.
		C≡C	J_{W-C}	C≡O	J_{W-C}	C≡O	C≡C	W=O	
1a	$[W(CO)(C_2H_2)L_2]$	200.0, 193.1	53, 2	235.3	145	1889	1588, 1566	–	[15]
1b	$[W(CO)(C_2Me_2)L_2]$	208.7, 200.2	57, 12	235.5	145	1880	1590, 1570	–	–
1c	$[W(CO)(C_2Ph_2)L_2]$	210.6, 208.9, 203.4, 192.5	53, 53, 16, 16	236.8, 235.7	140, 140	1927, 1894	1588, 1574, 1565	–	–
2a	$[WO(C_2H_2)L_2]$	152.9, 151.9	28, 36	–	–	–	1604, 1597	939	[15]
2b	$[WO(C_2Me_2)L_2]$	152.8, 148.5	12, 9	–	–	–	1599	934	–
2c	$[WO(C_2Ph_2)L_2]$	151.7, 148.5	n.d.[a]	–	–	–	1611, 1595	936	–

[a] n.d. = not detected after 16000 scans due to low solubility.

Photoinduced alkyne release

Previously, we have demonstrated the reversible, photoinduced release of the C_2H_2 molecule from $[WO(C_2H_2)(S\text{-}Phoz)_2]$ (**2a**) to yield $[WO(S\text{-}Phoz)_2]$ (**3**) (Scheme 2).[15] Similarly, $[WO(C_2Me_2)(S\text{-}Phoz)_2]$ (**2b**) and $[WO(C_2Ph_2)(S\text{-}Phoz)_2]$ (**2c**) were also found to be capable of an analogous alkyne release to afford complex **3** and C_2R_2. In all cases, reactivity is evidenced by a characteristic color change from pale yellow to deep purple when exposing their solutions to sunlight for 2 min (Scheme 2). The color change was most pronounced in complex **2b** and barely visible in complex **2c**. These qualitative observations suggest a faster alkyne release from complex **2b** than from complex **2a** and a very slow release from complex **2c**. In agreement with the qualitatively observed alkyne release rates, $[WO(S\text{-}Phoz)_2]$ (**3**) is best synthesized by 2-butyne release from complex **2b**. Yields could be increased from $<20\,\%$ from $[WO(C_2H_2)(S\text{-}Phoz)_2]$[15] to up to 75% by exposing solutions of complex **2b** to light while constantly removing the liberated 2-butyne by bubbling N_2 through the reaction mixture. As the 14-electron species **3** forms in light but also decomposes after prolonged exposure, a fast reaction is critical. The observed difference in alkyne release from the $[WO(C_2R_2)(S\text{-}Phoz)_2]$ (**2a–c**) complexes was quantitatively assessed by in situ ^{1}H NMR measurements (Figure 3). Samples of the oxo-alkyne complexes (3.3×10^{-3} mol L^{-1} in CD_2Cl_2) were irradiated with monochromatic UV light (362 nm) from a high-pressure mercury lamp. The sample was exposed to the irradiation for 150 ms and ^{1}H NMR spectra were recorded immediately after the lamp flash. The efficiency of the alkyne release was monitored by integration of the CH_2 resonances.

We assume that photodissociation of the alkynes from the W center is a monomolecular process and depends only on concentration of the complexes itself. Thus, first-order kinetics were applied to describe changes in ^{1}H NMR spectra during UV irradiation. Pseudo-first-order photodissociation rate constants for complexes **2a–c** were extracted from the least-square fit of the time-resolved ^{1}H NMR data (see the Supporting Information, Figures S4–S6). In all reactions, a maximum product formation was reached after, at most, 3000 ms of UV irradiation. This is probably due to the equilibrium between the highly localized alkyne release (only part of the NMR-active volume was irradiated) and diffusion along the NMR tube, which continuously supplies new unreacted alkyne adduct. From integration results, the following rate constants of 1.37×10^8 s^{-1} (**2a**), 1.97×10^8 s^{-1} (**2b**), and 4.6×10^7 s^{-1} (**2c**) were extracted. These in situ ^{1}H NMR results confirm the qualitatively observed efficiency of **2b** > **2a** > **2c**. To shed light on the microsecond photoinduced behavior of the W–oxo–alkyne complexes, we used transient absorbance spectroscopy to explore all three compounds at micromolar concentrations. The time profiles of the alkyne release of complexes **2a–c** show an instant change in absorbance (see the Supporting Information, Figure S7) on the timescale of our experiment. This indicates a submicrosecond (few ns) release of the alkyne from the complex upon laser irradiation (355 nm). Additionally, these changes in the absorbance of complexes **2a–c** after equienergetic laser pulses correspond to the rates of alkyne release determined earlier by ^{1}H NMR spectroscopy.

These ^{1}H NMR spectroscopy data suggest a correlation between the rate of the photoinduced release and the electronic properties of the alkyne. The electron-withdrawing properties

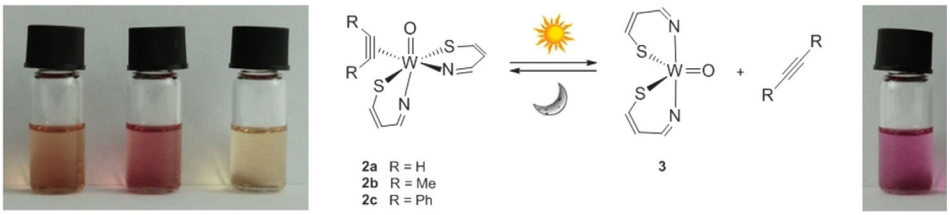

Scheme 2. Reversible behavior of the W–S-Phoz system towards light; S-Phoz ligand abbreviated for clarity. Left: solutions of complexes **2a**, **b**, and **c** after 2 min exposure to sunlight; Right: isolated complex **3** (CH_2Cl_2, 1 mg mL^{-1}).

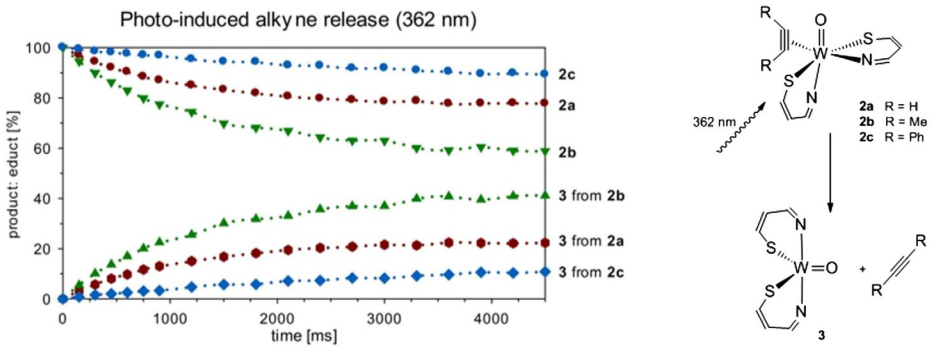

Figure 3. In situ ^{1}H NMR measurements. Comparison of the efficiency of the alkyne release from $[WO(C_2R_2)(S\text{-}Phoz)_2]$ (**2a–c**) complexes at 362 nm. S-Phoz ligand abbreviated for clarity.

of the phenyl substituents in complex **2c** are believed to cause a more pronounced metallacyclopropene character of the η^2-bound alkyne, thereby hindering its release. On the other hand, the electron-donating qualities of the methyl groups in complex **2b** might demand less backbonding from the W center to form a stable adduct, which would in turn facilitate the alkyne release. In the crystal structure of all W–alkyne complexes, the C≡C bonds are significantly elongated compared with the corresponding free alkyne bonds (C_2H_2 = 1.198(4),[31] C_2Me_2 = 1.211,[32] C_2Ph_2 = 1.18(6) Å).[33] Comparison of the elongation of the C≡C bonds upon coordination to the W center (molecular structures, see below) and observed photoinduced release suggests a correlation. Only complexes **2a** and **2b** ($\Delta_{C\equiv C_{coord}-C\equiv C_{free}}$ = 0.088 and 0.074 Å, respectively) with significant η^2-adduct character are adept to a fast photochemical alkyne release, whereas increasing metallacyclopropene character, as observed in complex **2c** ($\Delta_{C\equiv C}$ = 0.099 Å), leads to a significantly slower release. No photoreactivity was observed in the carbonyl complexes (**1a–c**), which exhibit a pronounced metallacyclopropene character. In the literature, several reports on the photoinduced release of small substrates ("*guests*") from their parent molecules ("*hosts*, *cages*") exist. This principle is currently under investigation for a wide array of applications, including targeted drug delivery.[34] The release of small, biologically relevant molecules, such as CO, H_2O_2, H_2S, and NO, by application of light has been shown.[35] However, a targeted alkyne release has not been reported so far, which makes our W–S-Phoz system the first example of a fully characterized system that is capable of a targeted and reversible release of acetylene, 2-butyne, and diphenylacetylene.

Oxidation products

We were also interested to determine whether the W–S-Phoz system can be oxidized further to W^{VI}, as such information is highly valuable for the understanding of nature's choice of oxidation states. Thus, [W^{IV}O(S-Phoz)$_2$] (**3**) was reacted in diethyl ether with one equivalent of PyNO for the formation of [WO_2(S-Phoz)$_2$] (**4**), as shown in Scheme 3. This resulted in an immediate color change from purple to deep yellow, and after workup, 40% of an air- and moisture-sensitive microcrystalline product was obtained. The ^{1}H NMR spectrum at room temperature exhibited only broad signals so that variable-temperature (VT) ^{1}H NMR experiments were performed. At −55 °C three sets of resonances are observed, which can be assigned to the three possible isomers of *cis*-dioxo [WO_2(S-Phoz)$_2$] (**4**): asymmetric *S,N-trans* (Figure 4, left) and symmetric *S,S-* and *N,N-trans* in the ratio 1:1:0.6. The dd (doublet of doublets) resonances of their CH_2 groups are shown in Figure 4, and their assignment was confirmed by ^{1}H,^{1}H COSY measurements at −55 °C (see the Supporting Information, Figure S2). The signals of the symmetric complexes were assigned by comparison of these CH_2 shifts to those of isomerically pure *S,S-trans* [$WO(C_2H_2)$(S-Phoz)$_2$] (**2a**) and *N,N-trans* [$W(CO)(C_2H_2)$(S-Phoz)$_2$] (**1a**) because of the close structural similarity.[15] Thus, the downfield-shifted set of signals at 4.50 and 4.26 ppm is believed to belong to the *N,N-trans* isomer, whereas the set at 3.87 and 2.44 ppm remain for the *S,S-trans* isomer. FTIR and EI-MS measurements further support the formation of the desired [WO_2(S-Phoz)$_2$] (**4**). The IR spectrum showed two terminal W=O stretches at 923 and 884 cm^{-1}, and the mass spectrum contained characteristic *m/z* peaks for [WO_2L_2] and [WO_2L]. Single-crystal X-ray diffraction analysis ultimately confirmed the compound to be complex **4**. Elemental analysis data were hampered by the pronounced sensitivity. The occurrence of all three possible isomeric forms in [WO_2L_2] complexes strongly supports the assignment of a mononuclear, octahedral, *cis*-dioxo structure for [WO_2(S-Phoz)$_2$] (**4**) in solution. Furthermore, the VT-NMR experiment demonstrates the highly dynamic behavior of the S-Phoz ligand system, which has been previously observed for

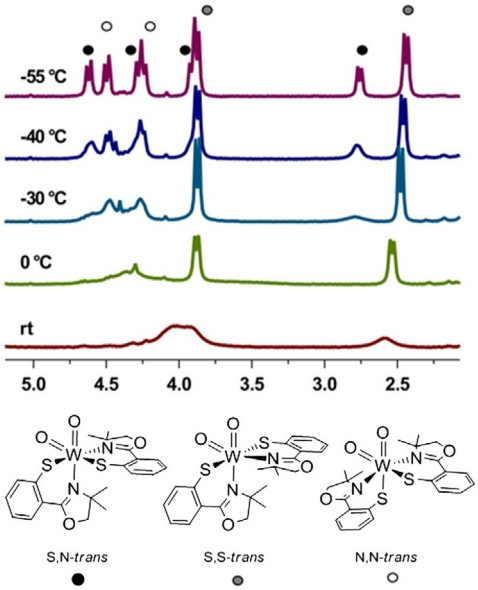

Figure 4. CH_2 region of variable-temperature ^{1}H NMR spectra of [WO_2(S-Phoz)$_2$] (**4**) in CD_2Cl_2. See the Supporting Information, Figure S1 for full spectra.

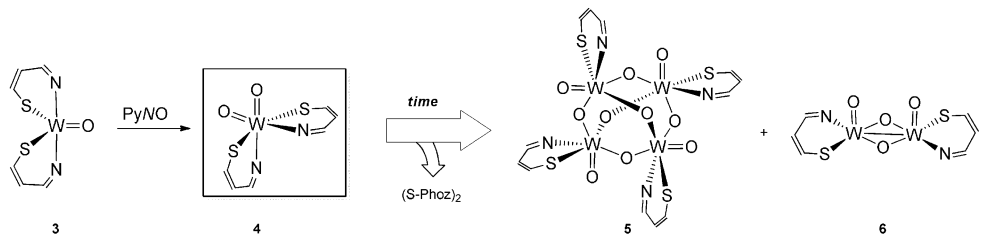

Scheme 3. Behavior of the W–S-Phoz system towards oxidation; S-Phoz ligand abbreviated for clarity.

$[W(CO)(C_2Ph_2)(S\text{-}Phoz)_2]$ (**1 c**, see above) and Pd^{II}–S-Phoz complexes.[29]

Over time, $[WO_2(S\text{-}Phoz)_2]$ (**4**) reacts to two additional ligand-containing complexes and disulfide $(S\text{-}Phoz)_2$, as shown in Scheme 3 and as monitored by ^1H NMR spectroscopy (see the Supporting Information, Figure S3). We were able to isolate them in small quantities (see the Supporting Information for procedure), which allowed their identification as the oxo compounds $[W_4O_4(\mu\text{-}O)_6(S\text{-}Phoz)_4]$ (**5**) and $[W_2O_2(\mu\text{-}O)_2(S\text{-}Phoz)_2]$ (**6**), as evidenced by single-crystal X-ray diffraction analyses (see below). For both compounds, ^1H NMR spectra reveal symmetric, diamagnetic species evidenced by only one set of ligand signals. Their IR spectra show tungsten oxo and tungsten μ-oxo stretching frequencies. Also, during the synthesis of $[WO(S\text{-}Phoz)_2]$ (**3**), the formation of compounds **5** and **6** is observed.

The mechanisms for their formation remain speculative, particularly the source of the two additional O atoms in complex **5**. However, it seems to be independent from O_2, as exposure of compounds **2 a**, **3**, and **4** to O_2 with and without light only resulted in the formation of $(S\text{-}Phoz)_2$ as the identifiable decomposition product observed by NMR spectroscopy. This points toward complex **3** being the source of the additional oxygen atoms. Isolation of larger quantities of complexes **4**–**6** is hampered by the fact that they are all light-sensitive, highly susceptible to hydrolysis, and rearrange in solution.

The understanding of these oxidation products is important in the overall context of the dioxygen sensitivity of the enzyme. The anaerobic enzyme AH loses its acetylene hydration activity when exposed to O_2.[2] Similar sensitivity is also observed with our complexes. While enzyme activity is restored by strong reducing agents like Ti^{III}citrate,[1] our system irreversibly forms $[W^{VI}{}_4O_4(\mu\text{-}O)_6(S\text{-}Phoz)_4]$ (**5**) and $[W^{V}{}_2O_2(\mu\text{-}O)_2(S\text{-}Phoz)_2]$ (**6**) and the disulfide $(S\text{-}Phoz)_2$. The investigation of the oxidation products also provides possible clues on the requirement of AH's natural oxidation state of +IV. In our system, the higher +VI oxidation state, which is common in Mo-dependent oxygen atom transfer enzymes, leads to labile species, not only towards acetylene activation but also towards aqueous conditions found in the enzyme. The lower +II state afforded too tightly bound metallacyclopropanes, which did not show the necessary degree of lability for further reactions. Furthermore, compounds **4**–**6** are interesting from a structural point of view as only four *cis*-WO_2 compounds with S,N or S_2,N_2-donor ligands, no $[W_4O_{10}]$-clusters, or $WO(\mu\text{-}O)_2OW$ motifs with S,N-ligands have been described, which hints at the elusiveness and instability of these systems.[36]

Molecular structures

Alkyne compounds

Molecular structures of the newly presented alkyne compounds (**1 b**, **1 c**, **2 b**, and **2 c**) were determined by single-crystal X-ray diffraction analysis. Selected bond lengths and angles are given in Table 2, and molecular views are presented in Figures 5 and 6. Compound **1 c** was crystallized in triclinic ($P\bar{1}$; depicted) and cubic ($I23$) arrangements. All compounds feature distorted octahedral environments around the W atom. The center of the alkyne C≡C bond occupies the sixth position, which is always located *cis* to the carbonyl or oxo groups. A significant loss of triple bond character and linearity is observed in all η^2-bound alkynes, which shows that the actual bonding situation is between the η^2-adduct and metallacyclopropene resonance structures. All bond lengths, angles, and

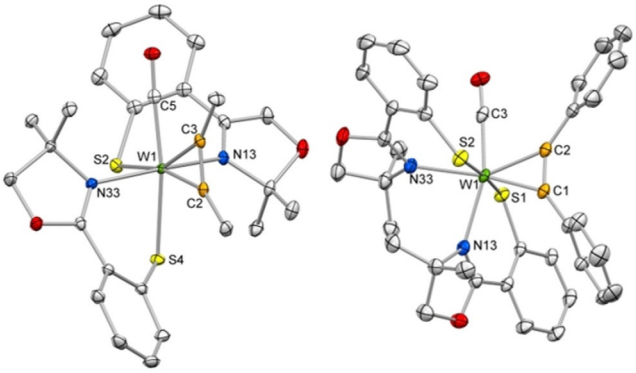

Figure 5. Molecular views of $[W(CO)(C_2Me_2)(S\text{-}Phoz)_2]$ (**1 b**, left) and $[W(CO)(C_2Ph_2)(S\text{-}Phoz)_2]$ (**1 c**, right) that show the atomic numbering scheme. Probability ellipsoids are drawn at the 50% level.

Table 2. Selected bond lengths [Å] and angles [°] of all presented compounds.

		C≡C	W–C≡C	≡C–R	R–C≡C	W–CO	WC≡O	W=O	W–(μ-O)	Ref.
1 a	N,N	1.327(3)	2.0548(18), 2.0268(17)	1.031(17), 1.031(17)	146.9(16), 122.7(15)	1.9623(18)	1.160(2)	–	–	[15]
1 b	N,N	1.314(3)	2.0210(17), 2.0565(17)	1.485(2), 1.482(2)	136.28(17), 139.03(17)	1.9535(19)	1.164(2)	–	–	–
1 c	S,S	1.305(6)	2.036(4), 2.057(4)	1.470(6), 1.463(6)	135.4(4), 137.3(4)	1.966(4)	1.154(5)	–	–	–
	S,S	1.309(3)	2.0510(19), 2.078(2)	1.463(3), 1.461(3)	142.8(2), 143.0(2)	1.949(2)	1.155(3)	–	–	–
2 a	S,S	1.268(6)	2.094(4), 2.109(4)	0.92(3), 0.92(3)	143(4), 149(3)	–	–	1.724(3)	–	[15]
2 b	S,S	1.285(3)	2.109(4), 2.120(4)	1.494(3), 1.484(3)	143.8(2), 144.0(2)	–	–	1.7148(14)	–	-
2 c	S,S	1.297(5)	2.102(2), 2.107(2)	1.465(5), 1.471(5)	141.9(4), 141.1(4)	–	–	1.714(3)	–	–
4	S,N	–	–	–	–	–	–	1.733(2), 1.728(2)	–	–
5	S,μO	–	–	–	–	–	–	1.711(16), 1.7264(16)	1.7713(15), 1.9266(7), 2.1287(15)[a]	–
6	S,μO	–	–	–	–	–	–	1.7085(19)	1.9237(16)	–

[a] Representative selection of the six observed bond lengths.

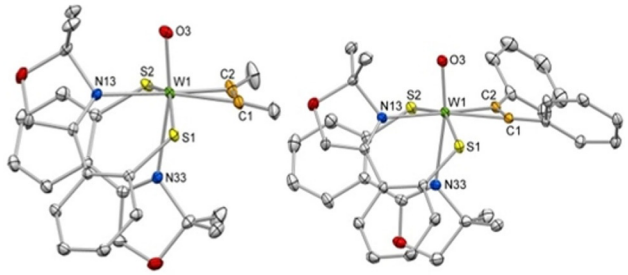

Figure 6. Molecular views of $[WO(C_2Me_2)(S\text{-}Phoz)_2]$ (**2b**, left) and $[WO(C_2Ph_2)(S\text{-}Phoz)_2]$ (**2c**, right) that show the atomic numbering scheme. Probability ellipsoids are drawn at the 50% level.

W–alkyne distances in complexes **1b** and **1c** are within the range previously observed in scorpionate-based W–carbonyl complexes.[37] Oxidation of the W–CO species results in an increased W–alkyne distance, which corresponds to a shift towards a more η^2-adduct-like structure and a less tightly bound alkyne. In contrast to the previously published C_2H_2 adduct **1a**, the introduction of the oxo ligand has little (**1b**) or no (**1c**) influence on the alkyne C≡C and C–R bond lengths.[15] The structure of complex **2b** represents only the second example of a W–oxo–C_2Me_2 adduct, next to $[WO(Tp')(H_2O)(C_2Me_2)][CF_3SO_3]$, for which a marginally shorter C≡C bond and a comparable W–alkyne distance (1.278(5) and 2.090(3) Å vs. 1.314(3) and 2.0210(17)/2.0565(17) Å) have been reported.[21] In complex **2c**, all bond lengths, angles, and W–alkyne distances are within the expected range of monomeric W–oxo–C_2Ph_2 adducts.[38] The first coordination spheres of the carbonyl (**1b**,**c**) and oxo species, (**2b**,**c**) show two major differences. In the carbonyl complexes, the alkyne C≡C bond is arranged parallel to the C≡O bond that is typical for group IV, d^4 alkyne complexes.[27] Upon oxidation, a 90° alkyne rotation is observed, which enables a perpendicular arrangement of the C≡C bond and the W=O group. We have observed this behavior previously in the C_2H_2 analogue, and it is consistent with literature.[15,21] Additionally, *S,S-trans* (C_2Ph_2) and *N,N-trans* (C_2Me_2) isomers were obtained. The CO compounds are believed to exist as isomeric mixtures (Scheme 1, see above), whereas all W–oxo compounds were obtained as pure *S,S-trans* isomers, with the N atom *trans* to the oxo group only weakly coordinated.

Oxidation products

Molecular structures of the oxidation products $[WO_2(S\text{-}Phoz)_2]$ (**4**), $[W_4O_4(\mu\text{-}O)_6(S\text{-}Phoz)_4]$ (**5**), and $[W_2O_2(\mu\text{-}O)_2(S\text{-}Phoz)_2]$ (**6**) were determined by single-crystal X-ray diffraction analysis. Molecular views are presented in Figure 7, and selected bond lengths and angles are given in Table 2. Regarding complex **5**, molecular structures of two different single crystals were determined, which were found to be virtually identical complexes in different packings. The dioxo compound $[WO_2(S\text{-}Phoz)_2]$ (**4**) was found to crystallize in a distorted octahedral geometry. The two thiophenolate ligands are coordinated in the asymmetric *S,N-trans* form with one nitrogen and one sulfur atom *trans* to an oxo group (N33-W1-O2 171.86(8)°, S1-W1-O1 164.21(7)°). The W–N33 and W–S1 bonds *trans* to the oxo moieties are typically elongated compared with the W–N and W–S bonds *trans* to each other. However, the W–O bond lengths are only slightly influenced by the different *trans* donors (1.733(2) and 1.728(2) Å). This isomer is also observed in solution, where it represents approximately 38% next to the *S,S-* and *N,N-trans* isomers (Figure 4). The occurrence of the asymmetric isomer is interesting as it has never been observed before in the W–S-Phoz system.[15] Furthermore, in molybdenum dioxo complexes with various phenolate-oxazoline ligands, only symmetric isomers were observed.[39] In $[W_4O_4(\mu\text{-}O)_6(S\text{-}Phoz)_4]$ (**5**), each of the distorted octahedral W^{VI} centers is surrounded by one bidentate S-Phoz, one terminal oxygen, and three bridging O atoms. The complex lies around a twofold rotation axis through the atoms O10 and O20, which leads to equal W–O bond lengths to these atoms (W1/W1′–O10 1.9266(7) Å, W2/W2′–O20 1.9122(7) Å). The other W–O distances within the W_4O_6 cluster are rather different. The short distances (e.g., W1–O12 1.7713(15) Å) are very similar to those of the terminal oxo groups (W1–O1 1.711(16) Å). The longer ones (e.g., W2–O12 2.1287(15) Å) are within the typical range of μ-oxo bridges. Thus, tetrameric **5** can be described as a dimer of $[W_2O_2(\mu\text{-}O)_2(S\text{-}Phoz)_2]$ dimers (see the Supporting Information, Figure S17). One W_4O_6-cluster has been published previously. Equivalent dimeric–dimer behavior has been observed, which results in comparable bond lengths and angles.[40] $[W_2O_2(\mu\text{-}O)_2(S\text{-}Phoz)_2]$ (**6**) features distorted square pyramidal W^V centers with the terminal O atom occupying the apex of the pyramid.

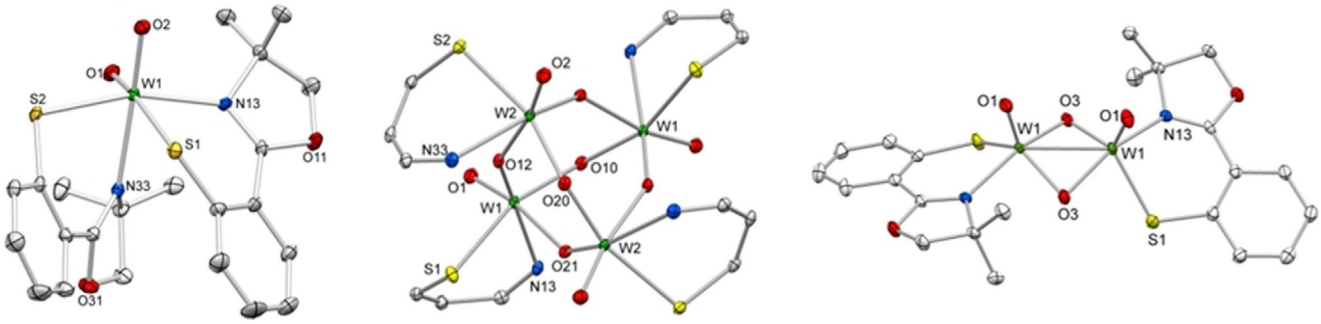

Figure 7. Molecular views of $[WO_2(S\text{-}Phoz)_2]$ (**4**, left), $[W_4O_4(\mu\text{-}O)_6(S\text{-}Phoz)_4]$ (**5**, middle), and $[W_2O_2(\mu\text{-}O)_2(S\text{-}Phoz)_2]$ (**6**, right) that show the atomic numbering scheme. For tetrameric **5**, the ligand's backbone was omitted for clarity. Probability ellipsoids are drawn at the 50% level.

The $WO(\mu\text{-}O)_2OW$ motif has been described previously, with most examples featuring five-coordinate W centers, but distorted octahedral arrangements have also been reported.[41] As observed in complex **6**, a *syn*-arrangement of the two terminal oxo groups seems to be preferred. Acid-catalyzed isomerization to the *anti* configuration has been reported.[42] The lengths of the terminal W=O and W–(μ-O) bonds observed in complex **6** are within the expected range.[41–43]

Conclusion

By using the S-Phoz ligand, we have successfully developed a synthetic protocol for the η^2-coordination of the alkynes C_2H_2, C_2Me_2, and C_2Ph_2 on bio-inspired W^{II}-bis-carbonyl centers to yield $[W(CO)(C_2R_2)(S\text{-}Phoz)_2]$ (**1a–c**). The introduction of an oxygen atom to yield $[WO(C_2R_2)(S\text{-}Phoz)_2]$ (**2a–c**) allowed access to the biological oxidation state of W^{IV} and the oxidation state W^{VI}. Additionally, the oxidation causes a decreased coordination of the alkynes, whilst leaving them significantly activated for further reactions. This is best reflected in the capability of the oxo complexes **2a–c** to reversibly release their alkyne from their metal center upon irradiation with UV light to afford five-coordinate $[WO(S\text{-}Phoz)_2]$ (**3**).

The W^{IV} species **3** was found to be prone to further oxidation to $[WO_2(S\text{-}Phoz)_2]$ (**4**) and ultimate rearrangement to the W^{VI} tetramer **5** and the W^{V} dimer **6**. This behavior is similar to the oxygen sensitive W center in AH and a good indication as to why native AH is only active, when present in the +IV state.

The observed *cis*-dioxo, oxo-(bis-μ-oxo), and oxo-tris-(μ-oxo) motifs have remained largely elusive in high-valent W chemistry with bio-inspired S-donor ligands. Moreover, we found that the rate of the reversible photoinduced alkyne release is closely correlated to the molecular structure of the W complex. This release, to the best of our knowledge, has never been described before and opens new possibilities for the design of novel photoswitchable enzymatic systems. Although the S-Phoz system is prone to hydrolysis and can therefore only be considered as a structural model of AH, complex **2a** shows the degree of lability of the acetylene group that is necessary for catalysis. Thus, their characterization is expected to further help in the design of a targeted synthesis of biomimetic W^{IV} and W^{VI} model complexes.

Experimental Section

Information regarding spectral characterization, VT- and in situ NMR measurements, transient absorbance spectroscopy, and crystallographic data and structure refinement are provided in the Supporting Information. CCDC 1868876 (**1b**), 1868877 (**1c**), 1868878 (**1c′**), 1868879 (**2b**), 1868880 (**2c**), 1868881 (**4**), 1868882 (**5**), 1868883 (**5′**), and 1868884 (**6**) contain the supplementary crystallographic data. These data can be obtained free of charge by The Cambridge Crystallographic Data Centre. All manipulations were performed under an atmosphere of N_2 by using standard Schlenk and glovebox techniques. LiS-Phoz, $[W(CO)_2(S\text{-}Phoz)_2]$, $[W(CO)(C_2H_2)(S\text{-}Phoz)_2]$ (**1a**) and $[WO(C_2H_2)(S\text{-}Phoz)_2]$ (**2a**) were synthesized according to our previously published protocol.[15,23] Pyridine-*N*-oxide was sublimated under vacuum. Diphenylacetylene was recrystallized from EtOH. 2-Butyne was dried over molecular sieves. Silica was washed with NEt_3 and dried at 110 °C prior to use.

Synthesis of $[W(CO)(C_2Me_2)(S\text{-}Phoz)_2]$ (1b)

$[W(CO)_2(S\text{-}Phoz)_2]$ (1.500 g, 2.30 mmol) was dissolved in CH_2Cl_2 (15 mL) and 2-butyne (0.901 mL, 11.50 mmol) was added. After stirring the mixture at 40 °C for 15 h, silica (1.5 g) was added and the mixture was stirred for 10 min. The solution was filtered, concentrated, and heptane was added to precipitate the product. After filtration and washing with heptane, the dark green, microcrystalline product was obtained in 76% yield (1.193 g, 1.76 mmol). Single crystals suitable for X-ray diffraction analysis were obtained from CH_2Cl_2/heptane solutions at −35 °C. ^{1}H NMR (300 MHz, CD_2Cl_2): δ = 7.76 (dd, J = 8.0, 1.0 Hz, 1H, Ar-H), 7.65 (dd, J = 7.9, 1.3 Hz, 1H, Ar-H), 7.61 (dd, J = 7.9, 0.9 Hz, 1H, Ar-H), 7.43 (dd, J = 8.0, 1.4 Hz, 1H, Ar-H), 7.31 (td, J = 7.6, 1.5 Hz, 1H, Ar-H), 7.17 (ddd, J = 8.0, 7.2, 1.6 Hz, 1H, Ar-H), 7.07 (td, J = 7.9, 1.3 Hz, 1H, Ar-H), 6.89 (ddd, J = 8.3, 7.2, 1.3 Hz, 1H, Ar-H), 4.17 (d, J = 8.3 Hz, 1H, CH_2), 4.04–3.88 (m, 3H, CH_2), 2.90 (s, 3H, C_2Me_2), 2.46 (s, 3H, C_2Me_2), 1.67 (s, 3H, Me), 1.41 (s, 3H, Me), 0.77 (s, 3H, Me), 0.58 ppm (s, 3H, Me); ^{13}C NMR (75 MHz, CD_2Cl_2): δ = 235.45 (J_{W-C} = 144.9 Hz, C≡O), 208.68 (J_{W-C} = 57.0 Hz, C_2Me_2), 200.18 (J_{W-C} = 11.4 Hz, C_2Me_2), 169.44 (Cq), 168.14 (Cq), 157.63 (Cq), 154.54(Cq), 134.41 (CH_{ar}), 131.95 (CH_{ar}), 131.10 (CH_{ar}), 130.99 (CH_{ar}), 130.63 (2 CH_{ar}), 130.04 (Cq), 128.72 (Cq), 123.22 (CH_{ar}), 121.81 (CH_{ar}), 79.84 (CH_2), 79.27 (CH_2), 76.12 (Cq), 74.21 (Cq), 28.50 (d, J = 1.9 Hz, Me), 27.72 (Me), 27.06 (Me), 26.50 (Me), 20.38 (C_2Me_2), 18.68 ppm (d, J = 1.5, C_2Me_2); IR: $\tilde{\nu}$ = 1880 (s, C≡O), 1590 (s, C≡C), 1570 (s, C≡C), 1540 cm^{-1} (m, C=N); MS (EI): m/z: 678.3 [M^+], 650.3 [M−CO]; elemental analysis calcd (%) for $C_{27}H_{30}N_2O_3S_2W$ (678.51): C 47.80, H 4.46, N 4.13, S 9.45; found: C 48.13, H 4.56, N 3.97, S 9.31.

Synthesis of $[W(CO)(C_2Ph_2)(S\text{-}Phoz)_2]$ (1c)

$[W(CO)_2(S\text{-}Phoz)_2]$ (1.000 g, 1.53 mmol) and diphenylacetylene (1.362 g, 7.64 mmol) were suspended in CH_2Cl_2. After stirring the mixture at 35 °C for 32 h, silica (1.1 g) was added, and the mixture was stirred for another 10 min. The solution was filtered, diluted with heptane (20 mL), and concentrated to precipitate the product. After filtration and washing with heptane (2×10 mL) the yellowish green, microcrystalline product was obtained in 67% yield (0.822 g, 1.02 mmol). Single crystals suitable for X-ray diffraction analysis were obtained from CH_2Cl_2/toluene/heptane solutions at −35 °C or CH_2Cl_2/heptane solutions at RT (cubic). ^{1}H NMR (300 MHz, CD_2Cl_2, two isomers in a 45:55 ratio): δ = 8.08 (dd, J = 8.2, 1.1 Hz, 1H, Ar-H), 7.88–7.83 (m, 1H, Ar-H), 7.81 (dd, J = 8.0, 1.2 Hz, 1H, Ar-H), 7.67 (d, J = 6.4 Hz, 1H, Ar-H), 7.59 (d, J = 8.0 Hz, 1H, Ar-H), 7.53–6.97 (m, 28H, Ar-H), 6.80–6.71 (m, 1H, Ar-H), 6.53–6.45 (m, 2H, Ar-H), 4.29 (d, J = 15.9 Hz, 1H, CH_2), 4.26 (d, J = 15.9 Hz, 1H, CH_2), 4.10–3.96 (m, 5H, CH_2), 3.85 (d, J = 8.3 Hz, 1H, CH_2), 1.84 (s, 3H, Me), 1.72 (s, 3H, Me), 1.45 (s, 6H, Me), 1.34 (s, 3H, Me), 1.29 (s, 3H, Me), 0.84 (s, 3H, Me), 0.76 ppm (s, 3H, Me); ^{13}C NMR (75 MHz, CD_2Cl_2): δ = 236.81 (J_{W-C} = 139.8 Hz, C≡O), 235.70 (J_{W-C} = 140.4 Hz, C≡O), 210.58 (J_{W-C} = 52.4 Hz, C_2Ph_2), 208.94 (J_{W-C} = 53.0 Hz, C_2Ph_2), 203.41 (J_{W-C} = 16.5 Hz, C_2Ph_2), 192.53 (J_{W-C} = 15.5 Hz, C_2Ph_2), 170.25 (Cq), 169.75 (Cq), 167.50 (Cq), 167.26 (Cq), 158.34 (Cq), 156.02 (Cq), 155.27 (Cq), 154.30 (Cq), 143.36 (Cq), 141.22 (Cq), 141.19 (Cq), 138.56 (Cq), 134.91 (CH_{ar}), 132.69 (CH_{ar}), 132.41 (CH_{ar}), 132.03, 131.75, 131.61, 131.47, 131.36, 131.25 (CH_{ar}), 130.97 (CH_{ar}), 130.60 (CH_{ar}), 130.46, 130.34 (CH_{ar}), 129.62, 129.19, 128.98, 128.86, 128.55, 128.49, 128.38, 128.30, 128.05, 127.98, 127.62, 126.71, 126.67, 125.84 (2 CH_{ar}), 124.11 (CH_{ar}), 123.58 (CH_{ar}), 123.17 (CH_{ar}), 121.87 (CH_{ar}), 80.32 (CH_2), 79.83 (CH_2), 79.65 (CH_2), 78.97 (CH_2),

76.58 (Cq), 76.10 (Cq), 75.24 (Cq), 74.59 (Cq),28.87 (Me), 28.34 (Me), 28.32 (Me), 27.96 (Me), 27.92 (Me), 27.06 (Me), 26.85 (Me), 24.24 ppm (Me); IR: $\tilde{\nu}$ = 1927 (s, C≡O), 1894 (s, C≡O), 1588 (s, C≡C), 1574 (sh, C≡C), 1565 (s, C≡C), 1543 (sh, C=N), 1532 cm^{-1} (m, C=N); MS (EI): No assignable signals; elemental analysis calcd (%) for $C_{37}H_{34}N_2O_3S_2W$ (802.65): C 55.37, H 4.27, N 3.49, S 7.99; found: C 55.47, H 4.43, N 3.27, S 7.66.

Dynamic behavior in solution (isomeric ratios): $CDCl_3$ (47:53), [D_6]DMSO (30:70), [D_8]THF (20:80), C_6D_6 (32:68), [D_3]MeCN (38:62).

Synthesis of [$WO(C_2Me_2)$(S-Phoz)$_2$] (2 b)

Pyridine-*N*-oxide (0.048 g, 0.51 mmol) dissolved in CH_2Cl_2 (1 mL) was added to a solution of [$W(CO)(C_2Me_2)$(S-Phoz)$_2$] (**1 b**) (0.344 g, 0.46 mmol) in CH_2Cl_2 (3 mL) and stirred at RT. After 1 h, the reaction mixture was evaporated to dryness and washed with diethyl ether (3×5 mL), dissolved in CH_2Cl_2/heptane, and evaporated to dryness to yield the product as pale yellow microcrystalline powder (0.221 g, 0.33 mmol, 65%). Single crystals suitable for X-ray diffraction analysis were obtained from CH_2Cl_2/toluene/heptane solutions at −35 °C. ^{1}H NMR (300 MHz, CD_2Cl_2): δ = 7.83 (d, *J* = 7.8 Hz, 1 H, Ar-H), 7.63–7.50 (m, 2 H, Ar-H), 7.45 (dd, *J* = 7.8, 1.2 Hz, 1 H, Ar-H), 7.39 (td, *J* = 7.7, 1.5 Hz, 1 H, Ar-H), 7.29 (td, *J* = 7.7, 1.6 Hz, 1 H, Ar-H), 7.14 (td, *J* = 7.8, 1.1 Hz, 1 H, Ar-H), 7.08–7.00 (m, 1 H, Ar-H), 3.86 (d, *J* = 8.1 Hz, 1 H, CH_2), 3.39 (d, *J* = 8.1 Hz, 1 H, CH_2), 3.12 (s, 3 H, C_2Me_2), 3.00 (s, 3 H, C_2Me_2), 2.51 (d, *J* = 8.1 Hz, 1 H, CH_2), 2.00 (d, *J* = 8.1 Hz, 1 H, CH_2), 1.75 (s, 3 H, Me), 1.29 (s, 3 H, Me), 0.98 (s, 3 H, Me), 0.60 ppm (s, 3 H, Me); ^{13}C NMR (75 MHz, CD_2Cl_2): δ = 165.62 (Cq), 164.94 (Cq), 154.57 (Cq), 154.46 (Cq), 152.82 (J_{W-C} = 11.2 Hz, C_2Me_2), 148.48, (J_{W-C} = 9.1 Hz, C_2Me_2), 135.78 (CH_{ar}), 134.38 (CH_{ar}), 132.02 (CH_{ar}), 131.25 (CH_{ar}), 129.92 (CH_{ar}), 129.64 (CH_{ar}), 129.50 (Cq), 128.12 (Cq), 123.72 (CH_{ar}), 123.60 (CH_{ar}), 77.85 (CH_2), 76.66 (CH_2), 75.22 (Cq), 71.61 (Cq), 28.73 (Me), 28.16 (Me), 21.84 (Me), 20.95 (Me, d, *J* = 1.9 Hz), 15.17 (C_2Me_2), 14.12 ppm (C_2Me_2); IR: $\tilde{\nu}$ = 1599 (s, C≡C), 1576 (w, C=N), 1549 (w, C=N), 934 cm^{-1} (s, W=O); MS (EI): *m/z*: 612.4 [*M*−C_2Me_2]; elemental analysis calcd (%) for $C_{26}H_{30}N_2O_3S_2W{\cdot}0.4\,CH_2Cl_2$ (700.48): C 45.27, H 4.43, N 4.00, S 9.15; found: C 45.35, H 4.42, N 4.08, S 9.31.

Synthesis of [$WO(C_2Ph_2)$(S-Phoz)$_2$] (2 c)

Pyridine-*N*-oxide (0.048 g, 0.51 mmol) dissolved in CH_2Cl_2 (1 mL) was added to a solution of [$W(CO)(C_2Ph_2)$(S-Phoz)$_2$] (**1 c**) (0.407 g, 0.46 mmol) in CH_2Cl_2 (3 mL) and stirred at RT. After 1 h, the reaction mixture was evaporated to dryness and washed with diethyl ether (2×5 mL). The residue was dissolved in CH_2Cl_2/heptane and evaporated to dryness to yield the product as yellow microcrystalline powder (0.225 g, 0.28 mmol, 62%). Single crystals suitable for X-ray diffraction analysis were obtained from CH_2Cl_2/toluene/heptane solutions at −35 °C. ^{1}H NMR (300 MHz, CD_2Cl_2): δ = 7.86–7.78 (m, 3 H, Ar-H), 7.70 (dd, *J* = 8.1, 1.1 Hz, 2 H, Ar-H), 7.61–7.37 (m, 9 H, Ar-H), 7.34–7.28 (m, 1 H, Ar-H), 7.25 (td, *J* = 7.8, 1.6 Hz, 1 H, Ar-H), 7.16 (td, *J* = 7.7, 1.1 Hz, 1 H, Ar-H), 7.09–7.02 (m, 1 H, Ar-H), 3.93 (d, *J* = 8.1 Hz, 1 H, CH_2), 3.43 (d, *J* = 8.1 Hz, 1 H, CH_2), 2.62 (d, *J* = 8.2 Hz, 1 H, CH_2), 2.03 (d, *J* = 8.1 Hz, 1 H, CH_2), 1.92 (s, 3 H, Me), 1.43 (s, 3 H, Me), 1.06 (s, 3 H, Me), 0.80 ppm (s, 3 H, Me); ^{13}C NMR (75 MHz, CD_2Cl_2): δ = 165.85 (Cq), 165.07 (Cq), 163.87 (Cq), 163.13 (Cq), 151.73 (C_2Ph_2), 148.45 (C_2Ph_2), 138.52 (Cq), 137.16 (Cq), 135.72 (CH_{ar}), 134.20 (CH_{ar}), 132.09 (CH_{ar}), 131.75 (2 CH_{ar}), 131.45 (CH_{ar}), 130.84 (2 CH_{ar}), 130.06 (CH_{ar}), 129.85 (CH_{ar}), 129.15 (Cq), 128.85 (2 CH_{ar}), 128.66 (CH_{ar}), 128.49 (2 CH_{ar}), 128.24 (CH_{ar}), 127.82 (Cq), 123.99 (CH_{ar}), 123.79 (CH_{ar}), 78.09 (CH_2), 76.99 (CH_2), 75.67 (Cq), 71.81 (Cq), 29.01 (Me), 28.16 (Me), 22.21 (Me), 20.99 ppm (Me); IR: $\tilde{\nu}$ = 1611 (s, C≡C), 1595 (s, C≡C), 1573 (w, C=N), 1548 (w, C=N), 936 cm^{-1} (s, W=O); MS (EI): *m/z*: 612.3 [*M*−C_2Ph_2]; elemental analysis calcd (%) for $C_{36}H_{34}N_2O_3S_2W{\cdot}0.5\,CH_2Cl_2$ (833.11): C 52.62, H 4.23, N 3.36, S 7.70; found: C 52.45, H 4.24, N 3.46, S 7.92.

Improved synthesis of [WO(S-Phoz)$_2$] (3)

[$WO(C_2Me_2)$(S-Phoz)$_2$] (**2 b**) (0.384 g, 0.58 mmol) was dissolved in CH_2Cl_2 (35 mL) in a Schlenk flask equipped with a bubbler, and the solution was irradiated with light under a continuous N_2 flow for 3 h. The reaction mixture was dried, suspended in MeCN (7 mL), and the insoluble fraction was isolated by filtration. Washing with MeCN (2×3 mL) afforded the product in 75% yield (0.252 g, 0.41 mmol). ^{1}H NMR (300 MHz, CD_2Cl_2): δ = 8.07 (dd, *J* = 7.9, 1.5 Hz, 2 H, Ar-H), 7.71 (dd, *J* = 7.7, 1.2 Hz, 2 H, Ar-H), 7.11 (dtd, *J* = 19.9, 7.3, 1.4 Hz, 4 H, Ar-H), 4.59 (d, *J* = 8.5 Hz, 2 H, CH_2), 4.39 (d, *J* = 8.5 Hz, 2 H, CH_2), 1.99 (s, 6 H Hz, Me), 1.42 ppm (s, 6 H, Me); ^{13}C NMR (75 MHz, CD_2Cl_2): δ = 161.33 (C_q), 159.39 (C_q), 133.57 (2 CH_{arom}), 132.79 (CH_{arom}), 123.98 (CH_{arom}), 121.87 (C_q), 78.28 (C_q), 77.85 (CH_2), 27.98 (Me), 25.41 ppm (Me); IR: $\tilde{\nu}$ = 1589 (m, C=N), 1569 (m, C=N), 934 cm^{-1} (s, W=O); MS (EI): *m/z*: 612.1 [M^+]; elemental analysis calcd (%) for $C_{22}H_{24}N_2O_3S_2W{\cdot}0.3\,CH_2Cl_2$ (637.88): C 41.99, H 3.89, N 4.39, S 10.05; found: C 41.72, H 3.86, N 4.40, S 10.32.

Synthesis of [WO_2(S-Phoz)$_2$] (4)

Pyridine-*N*-oxide (0.026 g, 27 mmol) was added to [WO(S-Phoz)$_2$] (**3**) (0.035 g, 0.06 mmol) suspended in diethyl ether (4 mL). After 3 min, the yellow suspension was filtered over a pad of Celite. The yellow product was eluted with CH_2Cl_2, precipitated with heptane, and isolated by filtration to afford a yellow microcrystalline powder in 40% yield. Single crystals suitable for X-ray diffraction analysis were obtained from CH_2Cl_2/heptane solutions at −35 °C. ^{1}H NMR (300 MHz, CD_2Cl_2, RT, three dynamic isomers): δ = 7.87–6.89 (m, 8 H, Ar-H), 4.38–3.71 (bd, *J* = 30 Hz Hz, 3 H, -CH_2-), 2.71–2.42 (s, 1 H, -CH_2-), 1.87–1.14 ppm (m, 12 H, Me); ^{1}H NMR (300 MHz, CD_2Cl_2, −55 °C, three isomers: *S,N-trans*/*S,S-trans*/*N,N-trans* = 1:1:0.6): δ = 7.77–7.06 (m, Ar-H), 6.69 (d, *J* = 7.8 Hz, Ar-H), 4.62 (d, *J* = 8.7 Hz, CH_2, *S,N-trans*), 4.50 (d, *J* = 8.6, CH_2, *N,N-trans*), 4.26 (t, *J* = 9.5 Hz, -CH_2, *S,N-* and *N,N-trans*), 3.89 (t, *J* = 9.3 Hz, CH_2, *S,N-* and *S,S-trans*), 2.76 (d, *J* = 8.1 Hz, CH_2, *S,N-trans*), 2.44 (d, *J* = 8.1, CH_2, *S,S-trans*), 1.88 (s, Me), 1.71 (s, Me), 1.65 (s, Me), 1.40 (s, Me), 1.39 (s, Me), 1.32 (s, Me), 1.27 ppm (s, Me); IR: $\tilde{\nu}$ = 923 (W=O), 884 cm^{-1} (W=O); MS (EI): *m/z*: 628.2 [M^+], 612.2 [*M*−O], 422.0 [*M*−L].

Acknowledgements

The authors would also like to thank Bernd Werner for performing VT-NMR spectroscopic measurements. The authors gratefully acknowledge financial support from the NAWI Graz.

Conflict of interest

The authors declare no conflict of interest.

Keywords: alkyne ligands · bioinorganic chemistry · photodissociation · sulfur · tungsten

[1] B. M. Rosner, B. Schink, *J. Bacteriol.* **1995**, *177*, 5767 – 5772.
[2] R. U. Meckenstock, R. Krieger, S. Ensign, P. M. H. Kroneck, B. Schink, *Eur. J. Biochem.* **1999**, *264*, 176 – 182.

[3] E.-M. Burger, S. La Andrade, O. Einsle, *Curr. Opin. Struct. Biol.* **2015**, *35*, 32 – 40.
[4] G. Seiffert, G. M. Ullmann, A. Messerschmidt, B. Schink, P. M. H. Kroneck, O. Einsle, *Proc. Natl. Acad. Sci. USA* **2007**, *104*, 3073 – 3077.
[5] a) P. M. H. Kroneck, *J. Biol. Inorg. Chem.* **2016**, *21*, 29 – 38; b) M. Boll, O. Einsle, U. Ermler, P. M. H. Kroneck, G. M. Ullmann, *J. Mol. Microbiol. Biotechnol.* **2016**, *26*, 119 – 137; c) R.-Z. Liao, J.-G. Yu, F. Himo, *Proc. Natl. Acad. Sci. USA* **2010**, *107*, 22523 – 22527; d) R.-Z. Liao, W. Thiel, *J. Comput. Chem.* **2013**, *34*, 2389 – 2397; e) M. A. Vincent, I. H. Hillier, G. Periyasamy, N. A. Burton, *Dalton Trans.* **2010**, *39*, 3816 – 3822; f) S. Antony, C. A. Bayse, *Organometallics* **2009**, *28*, 4938 – 4944.
[6] a) A. Majumdar, *Dalton Trans.* **2014**, *43*, 8990 – 9003; b) *Biomimetic Chemistry of Molybdenum* (Ed.: B. Meunier), Imperial College Press, London, **2000**; c) A. Majumdar, S. Sarkar, *Coord. Chem. Rev.* **2011**, *255*, 1039 – 1054.
[7] H. Sugimoto, H. Tsukube, *Chem. Soc. Rev.* **2008**, *37*, 2609 – 2619.
[8] a) P. Basu, S. J. N. Burgmayer, *J. Biol. Inorg. Chem.* **2015**, *20*, 373 – 383; b) C. Schulzke, *Eur. J. Inorg. Chem.* **2011**, 1189 – 1199; c) R. H. Holm, E. I. Solomon, A. Majumdar, A. Tenderholt, *Coord. Chem. Rev.* **2011**, *255*, 993 – 1015.
[9] a) L. J. Laughlin, C. G. Young, *Inorg. Chem.* **1996**, *35*, 1050 – 1058; b) Z. Xiao, M. A. Bruck, J. H. Enemark, C. G. Young, A. G. Wedd, *Inorg. Chem.* **1996**, *35*, 7508 – 7515; c) Z. Xiao, C. G. Young, J. H. Enemark, A. G. Wedd, *J. Am. Chem. Soc.* **1992**, *114*, 9194 – 9195.
[10] a) J. M. Berg, R. H. Holm, *J. Am. Chem. Soc.* **1985**, *107*, 925 – 932; b) J. M. Berg, R. H. Holm, *J. Am. Chem. Soc.* **1985**, *107*, 917 – 925; c) J. M. Berg, R. H. Holm, *J. Am. Chem. Soc.* **1984**, *106*, 3035 – 3036.
[11] B. E. Schultz, S. F. Gheller, M. C. Muetterties, M. J. Scott, R. H. Holm, *J. Am. Chem. Soc.* **1993**, *115*, 2714 – 2722.
[12] D. Dowerah, J. T. Spence, R. Singh, A. G. Wedd, G. L. Wilson, F. Farchione, J. H. Enemark, J. Kristofzski, M. Bruck, *J. Am. Chem. Soc.* **1987**, *109*, 5655 – 5665.
[13] S. K. Das, D. Biswas, R. Maiti, S. Sarkar, *J. Am. Chem. Soc.* **1996**, *118*, 1387 – 1397.
[14] M. Schreyer, L. Hintermann, *Beilstein J. Org. Chem.* **2017**, *13*, 2332 – 2339.
[15] L. M. Peschel, F. Belaj, N. C. Mösch-Zanetti, *Angew. Chem. Int. Ed.* **2015**, *54*, 13018 – 13021; *Angew. Chem.* **2015**, *127*, 13210 – 13213.
[16] T. W. Crane, P. S. White, J. L. Templeton, *Organometallics* **1999**, *18*, 1897 – 1903.
[17] J. L. Templeton, B. C. Ward, G. J.-J. Chen, J. W. McDonald, W. E. Newton, *Inorg. Chem.* **1981**, *20*, 1248 – 1253.
[18] a) J. Yadav, S. K. Das, S. Sarkar, *J. Am. Chem. Soc.* **1997**, *119*, 4315 – 4316; b) Y.-F. Liu, R.-Z. Liao, W.-J. Ding, J.-G. Yu, R.-Z. Liu, *J. Biol. Inorg. Chem.* **2011**, *16*, 745 – 752.
[19] L. Ricard, R. Weiss, W. E. Newton, G. J.-J. Chen, J. W. McDonald, *J. Am. Chem. Soc.* **1978**, *100*, 1318 – 1320.
[20] M. B. Wells, P. S. White, J. L. Templeton, *Organometallics* **1997**, *16*, 1857 – 1864.
[21] T. W. Crane, P. S. White, J. L. Templeton, *Inorg. Chem.* **2000**, *39*, 1081 – 1091.
[22] a) G. Mugesh, H. B. Singh, R. J. Butcher, *J. Chem. Res.* **1999**, 472 – 473; b) R. C. R. Bottini, R. A. Gariani, C. D. O. Cavalcanti, F. de Oliveira, N. D. L. G. da Rocha, D. Back, E. S. Lang, P. B. Hitchcock, D. J. Evans, G. G. Nunes, F. Simonelli, E. L. de Sá, J. F. Soares, *Eur. J. Inorg. Chem.* **2010**, 2476 – 2487.
[23] L. M. Peschel, J. A. Schachner, C. H. Sala, F. Belaj, N. C. Mösch-Zanetti, *Z. Anorg. Allg. Chem.* **2013**, *639*, 1559 – 1567.
[24] a) A. Chimiak, R. C. Hider, A. Liu, J. B. Neilands, K. Nomoto, Y. Sugiura in *Strukcture and Bonding. Siderophores from Microorganisms and Plants, Vol. 58* (Eds.: M. J. Clarke, J. B. Goodenough, J. A. Ibers, D. M. P. Mingos, J. B. Neilands, G. A. Palmer, D. Reinen, P. J. Sadler, R. Weiss, R. J. P. Williams), Springer, Berlin, **1984**, pp. 1 – 135; b) R. J. Bergeron, *Chem. Rev.* **1984**, *84*, 587 – 602.
[25] a) G. Mugesh, H. B. Singh, R. J. Butcher, *Eur. J. Inorg. Chem.* **2001**, 669 – 678; b) H. R. Hoveyda, S. J. Rettig, C. Orvig, *Inorg. Chem.* **1993**, *32*, 4909 – 4913; c) H. R. Hoveyda, V. Karunaratne, S. J. Rettig, C. Orvig, *Inorg. Chem.* **1992**, *31*, 5408 – 5416; d) Q.-L. Zhou, A. Pfaltz, *Tetrahedron Lett.* **1993**, *34*, 7725 – 7728; e) J. Sprinz, M. Kiefer, G. Helmchen, M. Reggelin, G. Huttner, O. Walter, L. Zsolnai, *Tetrahedron Lett.* **1994**, *35*, 1523 – 1526.
[26] a) P. K. Baker, M. M. Meehan, *Inorg. Chim. Acta* **2000**, *303*, 17 – 23; b) P. K. Baker, M. G. B. Drew, M. M. Meehan, H. K. Patel, A. White, *J. Chem. Res.* **1998**, 379; c) P. K. Baker, D. J. Muldoon, A. J. Lavery, A. Shawcross, *Polyhedron* **1994**, *13*, 2915 – 2921; d) M. Al-Jahdali, P. K. Baker, M. G. B. Drew, *J. Organomet. Chem.* **2001**, *622*, 228 – 241.
[27] J. L. Templeton in *Advances in Organometallic Chemistry. Four-Electron Alkyne Ligands in Molybdenum(II) and Tungsten(II) Complexes, Vol. 29*; (Eds.: F. G. A. Stone, R. West), Elsevier, San Diego, **1989**, pp. 1 – 100.
[28] N. L. Wieder, P. J. Carroll, D. H. Berry, *Organometallics* **2011**, *30*, 2125 – 2136.
[29] L. M. Peschel, C. Holzer, L. Mihajlović-Lalić, F. Belaj, N. C. Mösch-Zanetti, *Eur. J. Inorg. Chem.* **2015**, 1569 – 1578.
[30] a) J. R. Morrow, T. L. Tonker, J. L. Templeton, W. R. Kenan, *Organometallics* **1985**, *4*, 745 – 750; b) L. Carlton, J. L. Davidson, *J. Chem. Soc. Dalton Trans.* **1988**, 2071 – 2076.
[31] R. K. McMullan, Å. Kvick, P. Popelier, *Acta Crystallogr. Sect. B* **1992**, *48*, 726 – 731.
[32] E. Pignataro, B. Post, *Acta Crystallogr.* **1955**, *8*, 672 – 674.
[33] A. Mavridis, I. Moustakali-Mavridis, *Acta Crystallogr. Sect. B* **1977**, *33*, 3612 – 3615.
[34] D.-H. Qu, Q.-C. Wang, Q.-W. Zhang, X. Ma, H. Tian, *Chem. Rev.* **2015**, *115*, 7543 – 7588.
[35] C. Brieke, F. Rohrbach, A. Gottschalk, G. Mayer, A. Heckel, *Angew. Chem. Int. Ed.* **2012**, *51*, 8446 – 8476; *Angew. Chem.* **2012**, *124*, 8572 – 8604.
[36] a) Y.-L. Wong, A. R. Cowley, J. R. Dilworth, *Inorg. Chim. Acta* **2004**, *357*, 4358 – 4372; b) Y.-L. Wong, J.-F. Ma, W.-F. Law, Y. Yan, W.-T. Wong, Z.-Y. Zhang, T. C. W. Mak, D. K. P. Ng, *Eur. J. Inorg. Chem.* **1999**, 313 – 321; c) A. Thapper, O. Balmes, C. Lorber, P. H. Svensson, R. H. Holm, E. Nordlander, *Inorg. Chim. Acta* **2001**, *321*, 162 – 166; d) S. C. Lee, R. H. Holm, *Inorg. Chim. Acta* **2008**, *361*, 1166 – 1176; e) C. A. Rice, P. M. H. Kroneck, J. T. Spence, *Inorg. Chem.* **1981**, *20*, 1996 – 2000.
[37] a) S. G. Feng, A. S. Gamble, C. C. Philipp, P. S. White, J. L. Templeton, *Organometallics* **1991**, *10*, 3504 – 3512; b) C. J. Adams, A. Baber, S. Boonyuen, N. G. Connelly, B. E. Diosdado, A. Kantacha, A. G. Orpen, E. Patrón, *Dalton Trans.* **2009**, 9746 – 9758; c) C. J. Adams, N. G. Connelly, S. Onganusorn, *Dalton Trans.* **2009**, 3062 – 3073; d) C. J. Adams, I. M. Bartlett, S. Carlton, N. G. Connelly, D. J. Harding, O. D. Hayward, A. G. Orpen, E. Patron, C. D. Ray, P. H. Rieger, *Dalton Trans.* **2007**, 62 – 72; e) I. M. Bartlett, S. Carlton, N. G. Connelly, D. J. Harding, O. D. Hayward, A. G. Orpen, C. D. Ray, P. H. Rieger, *Chem. Commun.* **1999**, 2403 – 2404; f) M. B. Wells, J. E. McConathy, P. S. White, J. L. Templeton, *Organometallics* **2002**, *21*, 5007 – 5020.
[38] a) N. G. Bokiy, Y. V. Gatilov, Y. T. Struchkov, N. A. Ustynyuk, *J. Organomet. Chem.* **1973**, *54*, 213 – 219; b) C. Khosla, A. B. Jackson, P. S. White, J. L. Templeton, *Organometallics* **2012**, *31*, 987 – 994; c) J.-W. Yang, C.-S. Chen, H.-F. Dai, C.-H. Chen, W.-Y. Yeh, *J. Organomet. Chem.* **2011**, *696*, 1487 – 1489.
[39] a) P. Traar, J. A. Schachner, B. Stanje, F. Belaj, N. C. Mösch-Zanetti, *J. Mol. Catal. A* **2014**, *385*, 54 – 60; b) M. Bagherzadeh, L. Tahsini, R. Latifi, A. Ellern, L. K. Woo, *Inorg. Chim. Acta* **2008**, *361*, 2019 – 2024; c) M. Gómez, S. Jansat, G. Muller, G. Noguera, H. Teruel, V. Moliner, E. Cerrada, M. B. Hursthouse, *Eur. J. Inorg. Chem.* **2001**, 1071 – 1076.
[40] H. Choujaa, A. L. Johnson, G. Kociok-Köhn, K. C. Molloy, *Dalton Trans.* **2012**, *41*, 11393 – 11401.
[41] R. Hazama, K. Umakoshi, A. Ichimura, S. Ikari, Y. Sasaki, T. Ito, *Bull. Chem. Soc. Jpn.* **1995**, *68*, 456 – 468.
[42] P. Schreiber, K. Wieghardt, U. Floerke, H. J. Haupt, *Inorg. Chem.* **1988**, *27*, 2111 – 2115.
[43] a) B. Modec, P. Bukovec, *Inorg. Chim. Acta* **2015**, *424*, 226 – 234; b) S. Khalil, B. Sheldrick, *Acta Crystallogr. Sect. B* **1978**, *34*, 3751 – 3753; c) S. Ikari, Y. Sasaki, T. Ito, *Inorg. Chem.* **1990**, *29*, 53 – 56.

Manuscript received: November 13, 2018
Revised manuscript received: December 13, 2018
Version of record online: February 18, 2019

